Inelastic light scattering from inter-Landau level excitations in a two-dimensional electron gas

David Richards
Cavendish Laboratory, Madingley Road, Cambridge CB3 OHE, United Kingdom
(Received 29 October 1999)

Electronic magneto-Raman scattering measurements of a high-density two-dimensional electron gas are presented. At low magnetic field strengths, wave vector appears to be conserved in the Raman process, with the smooth evolution of the excitation spectrum of the electron gas from that of a two-dimensional system to the Landau quantized system observed, in good agreement with the behavior predicted by linear response theory. However, at higher field strengths two Raman scattering mechanisms appear to operate. A wave-vector-conserving mechanism allows the observation of charge-density excitations, and in particular of Bernstein modes, identified from a comparison with theory. The Bernstein mode is observed in depolarized Raman scattering with an intensity significantly greater than that predicted. Raman scattering with no conservation of wave vector also occurs from excitations involving changes in Landau level quantum number n of up to $\Delta n = 7$.

I. INTRODUCTION

Electronic Raman scattering has been demonstrated in recent years to be a powerful tool for the study of electron-electron interactions in the integer and fractional quantum Hall regimes of a two-dimensional electron gas (2DEG).[1–3] Yet despite the interest in the application of electronic Raman scattering to these complex systems, light scattering from quantum Hall states is still not well understood; in particular, breakdown of wave vector conservation is frequently invoked to explain the results of experiment. Even for the relatively simple system of a 2DEG at high filling factors, there have been relatively few reports of Raman scattering measurements, especially for the study of nonzero wave vector excitations.[4,5]

This paper reports a Raman study of the effect of magnetic field on a high-density 2DEG confined in a $GaAs/Al_{0.3}Ga_{0.7}As$ quantum well, exploring the evolution from a two-dimensional to a Landau quantized system, and the nature of electronic Raman scattering in the presence of a magnetic field. Angle-resolved Raman measurements have been performed for both zero and finite in-plane wave vector transfers to the 2DEG, with magnetic field strengths up to 6 T perpendicular to the plane of the 2DEG; for the electron density of the sample studied this corresponds to filling factors $\nu = hN/eB > 6$. The results of these experiments are compared with the results of calculations performed within the random phase approximation (RPA).

The transition to a Landau quantized 2D system can be characterized with Raman spectroscopy by measuring the single-particle excitation (SPE) spectrum of the electron gas, the form of which provides a clear signature of the dimensionality of the electrons.[5] For a 2DEG with no applied magnetic field the spectrum for SPE of wave vector change q has a characteristic asymmetric line shape, with a high-frequency cutoff at $v_F q$ (v_F is the Fermi velocity); for depolarized Raman scattering (measured with the polarizations of incident and scattered light orthogonal) the spin-flip SPE spectrum may be observed, whereas spin-conserving SPE may be observed in the polarized Raman spectrum (incident and scattered light polarizations parallel).[6,7] The ability to tune to a well-defined in-plane wave vector q, determined from the scattering geometry of the angle-resolved Raman experiment, results from the wave-vector-conserving nature of the Raman scattering process.[8]

A simple classical picture of the Landau quantization of the 2DEG involves the modification of the density of states (DOS) of the electron system as Landau levels form and the electrons are constrained to orbits in k space. For small magnetic fields such that $\omega_c < \Gamma$, where $\hbar\omega_c$ is the Landau level energy separation and $\hbar\Gamma$ is the broadening of the Landau levels, the system should behave essentially two dimensionally. For $\Gamma < \omega_c < v_F q$, the signature of the Landau quantized system—a series of discrete lines corresponding to transitions between Landau levels—will evolve out of the 2D SPE line shape as the magnetic field increases, with wave-vector-conserving transitions still possible between the different Landau level k-space orbits. At higher magnetic fields, such that $\omega_c > v_F q$, such wave-vector-conserving transitions will no longer be classically allowed. Of course, an accurate description of the SPE and collective excitations in a Landau quantized system requires an approach beyond this simple classical picture; such a scheme within the random phase approximation is outlined in Sec. II and then adopted throughout this work. Note that this approach does not include the effects of exchange and correlation but should, nevertheless, provide a reliable picture of the electronic excitation spectra for the small wave vectors probed experimentally.

Details of the Raman scattering experiments are provided in Sec. III and the results of measurements performed with weak magnetic fields are presented and analyzed in Sec. IV. Raman spectra obtained with slightly higher fields, such that the 2DEG is a well-defined Landau quantized system but still with $\hbar\omega_c \ll E_F$ (the Fermi energy), are presented in Sec. V. Experimental evidence, supported by RPA calculations, for the charge-density excitations in this system is given in Sec. VI and, finally, the role of breakdown in wave vector conservation in the Raman scattering process is considered in Secs. VII and VIII.

II. THEORY

The cross sections $R_\alpha(\mathbf{q},\omega)$ for Raman scattering by electronic excitations of energy ω and wave vector $\mathbf{q}$ in a semiconductor plasma may be described by the imaginary parts of the electronic response functions χ_α of the electron gas ($\alpha=0$ for SPE and ρ for charge-density excitations):[8]

$$R_\alpha(\mathbf{q},\omega)\propto -[N(\omega)+1]\mathrm{Im}[\chi_\alpha(\mathbf{q},\omega)], \tag{1}$$

where $N(\omega)$ is the Bose-Einstein occupation number. In fact, Eq. (1) is formally true only for nonresonant Raman scattering, whereas experiments are invariably performed under resonant conditions.[8] Nevertheless, this simple form has been shown to provide an excellent description of the Raman line shape for, e.g., spin-flip and non-spin-flip SPE,[7,9–11] and Landau-damped plasmons[12] in 2DEG systems.

Within the RPA, the charge-density response function χ_ρ is given by

$$\chi_\rho(\mathbf{q},\omega)=\frac{\chi_0(\mathbf{q},\omega)}{1-v(q)\chi_0(\mathbf{q},\omega)}, \tag{2}$$

where the electronic polarizability χ_0, the response function in the absence of the Coulomb interaction $v(q)$, describes Raman scattering from SPE. It should be noted that the RPA, which does not include exchange and correlation, is expected to fail for large wave vectors $q=|\mathbf{q}|$. However, for the moderate magnetic fields and small wave vectors considered here, it is expected to provide a reliable description of the excitation spectra of the 2DEG.

In calculations of the charge-density response χ_ρ, modifications to the 2D Coulomb interaction due to finite size effects of the quantum well are taken into account using the parametrization provided by Bulutay and Tomak,[13] and the effects of image charges in the sample surface are also included.[7]

In the absence of a magnetic field, χ_0 is given by the Lindhard sum:

$$\chi_0(\mathbf{q},\omega)=2\sum_{\mathbf{k}}\frac{f(E_{\mathbf{k}+\mathbf{q}},T)-f(E_{\mathbf{k}},T)}{E_{\mathbf{k}+\mathbf{q}}-E_{\mathbf{k}}-\hbar\omega-i\hbar\gamma}, \tag{3}$$

where $f(E_{\mathbf{k}},T)$ is the Fermi-Dirac occupation factor at temperature T for an electron state of wave vector $\mathbf{k}$ and energy E. γ is a phenomenological damping parameter.

For a 2DEG in the presence of a magnetic field, the sum over in-plane wave vectors $\mathbf{k}$ in Eq. (3) is changed to one over Landau levels, as the system becomes fully quantized:

$$\chi_0(\mathbf{q},\omega)=2\sum_{m,n}\frac{f(E_n,T)-f(E_m,T)}{E_n-E_m-\hbar\omega-i\hbar\gamma}|F_{m,n}(q)|^2. \tag{4}$$

This is a sum over all possible SPE's between Landau levels m and n, where the matrix elements $F_{mn}(q)$ are the overlap integrals of the Landau level wave functions[14–17]

$$|F_{m,n}(q)|^2=\frac{\min(m!,n!)}{\max(m!,n!)}\left(\frac{q^2l_0^2}{2}\right)^{|n-m|}\exp\left(\frac{-q^2l_0^2}{2}\right)\times\left[L_{\min(m,n)}^{|n-m|}\left(\frac{q^2l_0^2}{2}\right)\right]^2. \tag{5}$$

$l_0=\sqrt{\hbar/eB}$ is the magnetic length and L_m^n are the Laguerre polynomials.

As a finite phenomenological damping γ is included in the evaluation of $\chi_0(\mathbf{q},\omega)$ using Eqs. (3) and (4), a Mermin correction is applied to ensure particle number conservation:[18]

$$\chi_0^{\mathrm{M}}(\mathbf{q},\omega)=\frac{(1+i\gamma/\omega)\chi_0(\mathbf{q},\omega)}{1+i(\gamma/\omega)[\chi_0(\mathbf{q},\omega)/\chi_0(\mathbf{q},0)]}. \tag{6}$$

This Mermin-corrected polarizability $\chi_0^{\mathrm{M}}(\mathbf{q},\omega)$ is then employed in Eqs. (1) and (2). Note that γ is not necessarily the same as the broadening Γ of the Landau level density of states; $1/2\gamma$ is intended simply to represent the lifetime of single-particle states contributing to the free electron polarizability $\chi_0(\mathbf{q},\omega)$.

Nonparabolicity of the GaAs conduction band is taken into account in the determination of the Landau level energies E_n in Eq. (4) using the approach of Ekenberg:[19]

$$E_n(B)=\epsilon+(n+1/2)\frac{\hbar eB}{m^*}+[(8n^2+8n+5)\alpha+(n^2+n+1)\beta]\frac{e^2B^2}{2\hbar^2}. \tag{7}$$

The effective mass $m^*=0.0695$ and nonparabolicity parameters $\alpha=-2118\,\mathrm{eV\,\AA^4}$ and $\beta=-2684\,\mathrm{eV\,\AA^4}$ are defined through the dispersion of the quantum well conduction subband with electron wave vector $\mathbf{k}=(k_x,k_y)$,[7]

$$E(k)=\epsilon+\frac{\hbar^2k^2}{2m^*}+\alpha k^4+\beta k_x^2k_y^2. \tag{8}$$

Equation (8) is determined from a self-consistent solution of the Poisson and Schrödinger equations for the sample structure under investigation, using bulk nonparabolicity parameters.[20] For simplicity the spin splitting of the electron states is not included (except for $B=0$, see Ref. 10); except for small magnetic fields when the inversion asymmetry-induced spin splitting of the quantum well is significant,[21] over the magnetic field range considered here the Zeeman spin-splitting energy will be less than the energy between Landau levels.

III. EXPERIMENT

The sample investigated, which was also used for the work presented in Refs. 5,10, and 11, is an asymmetrically doped 180 Å wide $GaAs/Al_{0.3}Ga_{0.7}As$ quantum well with a 2DEG density of $\sim 1.3\times10^{12}\,\mathrm{cm^{-2}}$. Taking nonparabolicity into account through Eqs. (7) and (8), this density corresponds to a Fermi energy of 45 meV, which is kept constant in the calculations presented here.

Unless stated otherwise, the Raman spectra presented here were measured with incident and scattered polarizations orthogonal (depolarized scattering), with an excitation photon energy of 1.598 eV and incident power density of $\sim 1\,\mathrm{kW\,cm^{-2}}$. The sample was held in helium exchange gas in an Oxford Instruments Spectromag and oriented with the magnetic field $\mathbf{B}$ either perpendicular or at 45° to the plane

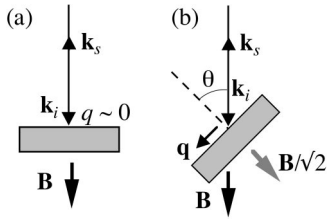

FIG. 1. Backscattering geometry for (a) the $\theta=0°$ orientation ($q=0$, $B_\perp=B$) and (b) the $\theta=45°$ orientation ($q=1.145\times10^5\,\mathrm{cm}^{-1}$, $B_\perp=B/\sqrt{2}$). $\mathbf{k}_{i(s)}$ is the wave vector of the incident (scattered) light.

of the quantum well. Raman measurements were performed in a backscattering configuration with the incident light wave vector parallel to **B**; this resulted in a Raman wave vector transfer $q=1.145\times10^5\,\mathrm{cm}^{-1}$ in the plane of the 2DEG for the 45° orientation and $q=0$ in the 0° case. The configurations of the two geometries are illustrated schematically in Fig. 1.

For the 45° orientation there are equal components of the magnetic field perpendicular to ($B_\perp$), and in ($B_\parallel$), the plane of the 2DEG; $B_\parallel=B_\perp=B/\sqrt{2}$. However, it is just the perpendicular component $B_\perp$ that leads to Landau quantization of the electron gas, although the electron spin is affected by the total magnetic field B. The parallel component $B_\parallel$ results in constant in-plane wave vector shifts of the quantum well subbands and is expected to have no effect on intrasubband (and, therefore, inter-Landau level) excitations. The intersubband energy of ~48 meV in the present sample (measurements of intersubband energies for a sample of similar structure are reported in Ref. 22) is sufficiently large that mixing between the first and second subbands, induced by $B_\parallel$,[23] is expected to have no effect in the energy range of interest studied here.

IV. LOW MAGNETIC FIELDS, $\omega_c < qv_F$

For $B=0$ and nonzero q (the 45° orientation), the characteristic double-peak structure for spin-flip single-particle excitations in the 2DEG was observed in the depolarized Raman spectrum, shown in Fig. 2(a), and the non-spin-flip SPE profile and the 2D plasmon were observed in the polarized spectrum (incident and scattered polarizations parallel).[7] A fit for the spin-flip SPE line shape, indicated by the thick black line in Fig. 2(b), was obtained from the electron polarizability using Eqs. (1), (3), and (6) with an electron temperature $T=40$ K, damping $\hbar\gamma=0.2$ meV, and taking full account of the quantum well conduction band spin splitting using the spin-splitting parameters determined in Ref. 10. Although the temperature indicated by the sample space thermometer was 10 K, an electron temperature of 40 K is not inconsistent with the form of the high-energy tail of the band-gap photoluminescence; given the high excitation energies and powers used in these experiments, this degree of heating of the electron gas is not unreasonable.[24] An electron temperature of 40 K will be assumed for all calculations presented here.

Depolarized Raman spectra measured in the 45° orientation for magnetic fields up to $B=2$ T (corresponding to $B_\perp=1.414$ T) are shown in Fig. 2(a). As the magnetic field is

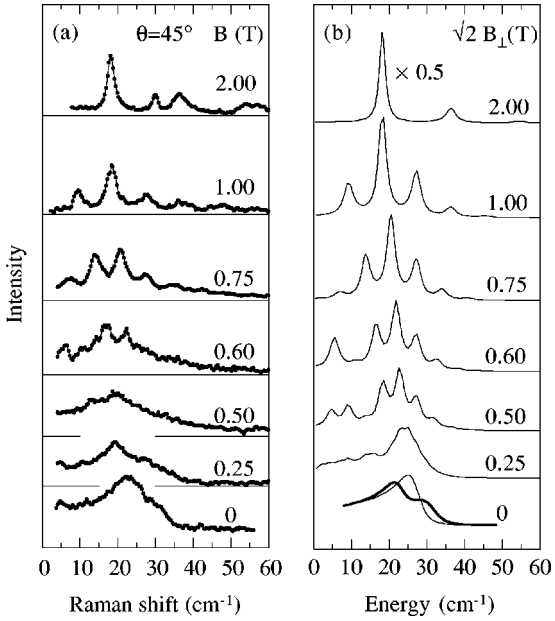

FIG. 2. (a) Depolarized Raman scattering spectra measured for low magnetic fields B in the 45° orientation ($q=1.145\times10^5\,\mathrm{cm}^{-1}$). The spin-flip SPE spectrum at $B=0$ is seen to evolve smoothly into the spectrum of inter-Landau level transitions with increasing magnetic field. The component of the magnetic field perpendicular to the plane of the 2DEG $B_\perp=B/\sqrt{2}$. (b) Theoretical SPE Raman spectra determined with Eq. (1) from the Mermin-corrected electon polarizability $\chi_0^{\mathrm{M}}(q,\omega)$ for various magnetic field strengths $B_\perp$ perpendicular to the plane of the 2DEG; for simplicity spin splitting has not been included in these calculations. However, for $B_\perp=0$ the spin-flip SPE spectrum is also shown (thick solid line), to enable comparison between theory and experiment. An electron temperature of 40 K and a damping of $\gamma=0.2$ meV have been assumed.

applied, the SPE peak shifts to lower energy and the high-frequency cutoff to higher energy. For $B\leqslant0.5$ T, the electron system can still be thought of as two-dimensional ($\omega_c<\Gamma$), reflected by the broad asymmetric band in the Raman spectrum. With increasing magnetic field a large number of peaks due to inter-Landau level excitations emerge smoothly out of the SPE signal, which preserves a broad asymmetric line shape up to $B\sim1$ T, suggesting within a semiclassical picture that in this regime ($\omega_c<qv_F$, the 2DEG SPE high-frequency cutoff) momentum-conserving transitions are still possible between the different Landau level k-space orbits.

SPE spectra calculated from the free electron polarizability χ_0 for $q=1.145\times10^5\,\mathrm{cm}^{-1}$, using Eqs. (1), (4), and (6), are shown in Fig. 2(b); for $0.6\,\mathrm{T}\leqslant B\leqslant1$ T there is excellent agreement between experiment and theory, with the relative intensities of the different inter-Landau level transitions well described by the overlap matrix elements for the Landau level wave functions given in Eq. (5). The discrepancies between theory and experiment for $B\leqslant0.5$ T can be attributed to the fact that spin splitting has not been included in these calculations.

However, agreement is not so good for $B=2$ T. For such a magnetic field $\omega_c\sim qv_F$ and momentum-conserving transitions between different Landau level k-space orbits will no longer be possible. In consequence, the theoretical Raman spectrum indicates a rapid decrease in intensity of the inter-

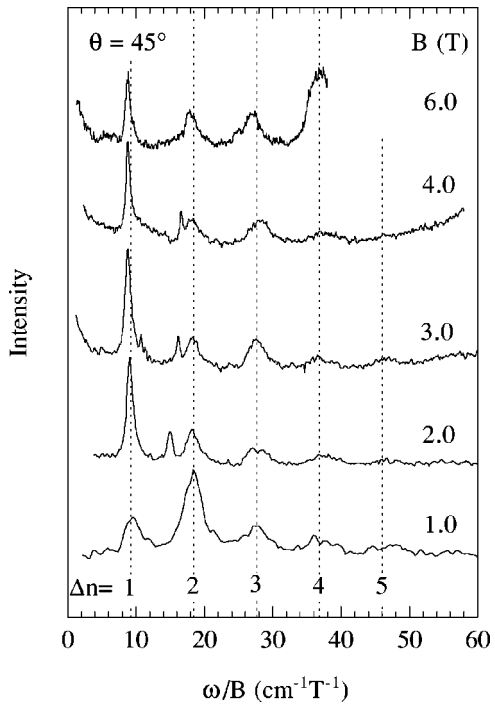

FIG. 3. Depolarized Raman scattering spectra measured in the 45° orientation. The component of the magnetic field perpendicular to the plane of the 2DEG $B_\perp = B/\sqrt{2}$. The Raman shift ω has been normalized by the magnetic field B (i.e., effectively normalized by the cyclotron frequency) to facilitate comparison between the different spectra.

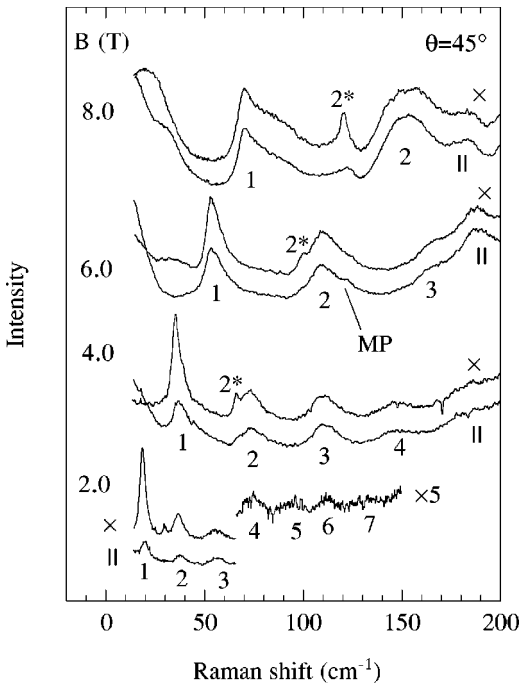

FIG. 4. Depolarized ($\times$, incident and scattered polarizations orthogonal) and polarized ($\|$, polarizations parallel) Raman scattering spectra measured in the 45° orientation. Numbers below peaks indicate the change Δn in Landau level index for inter-Landau level transitions. The narrow peak 2* below the $\Delta n = 2$ transition is assigned to a Bernstein mode. A shoulder (MP) on the high-energy side of the $\Delta n = 2$ peak observed at 6 T is assigned to the magnetoplasmon.

Landau level peaks with increasing order Δn, contrary to experimental observation.

V. MODERATE MAGNETIC FIELD, $qv_F < \omega_c \ll E_F/\hbar$

Raman spectra measured in the 45° orientation for 1 T $\leqslant B \leqslant 8$ T, corresponding to filling factors $50 \geqslant \nu \geqslant 6$, are shown in Figs. 3 and 4. From Fig. 3, where the spectra are shown as a function of a reduced Raman shift $\omega/B = (e/m_c^*)\omega/\sqrt{2}\omega_c$ (ω is the Raman shift and m_c^* is a cyclotron effective mass), it is readily apparent that the energies of the main equally spaced peaks in the spectra increase linearly with magnetic field, and hence cyclotron frequency $\omega_c = eB_\perp/m_c^*$. It is therefore natural to assign this series of peaks, for which Δn up to 7 are observed at low B, to inter-Landau level SPE's, the energies of which will vary as $\Delta n \hbar \omega_c$. This assignment is supported by a comparison of the peak energies with those determined from the peaks of the SPE Raman spectra calculated from χ_0^{M}, shown in Fig. 5 as a function of $B_\perp = B/\sqrt{2}$. Excellent agreement is obtained between the experimental and theoretical fan plots, with no free fitting parameters (except for the electron density which was determined from the $B = 0$ experimental plasmon energy; the electron temperature and phenomenological damping γ, determined from the $B = 0$ SPE line shape, have negligible effect on the theoretical SPE peak energies); the effects of nonparabolicity on the Landau level energies have been taken into account by Eq. (7). In addition to the inter-Landau level peaks, there is also a prominent narrow peak 2* present on the low-energy side of the $\Delta n = 2$ peak (see, e.g., Fig. 4); we will return to a discussion of the origin of this mode in Sec. VI.

Before further analysis, the origin of the inter-Landau level peaks should first be confirmed as Raman scattering from the 2DEG. For in a magneto-Raman study of a GaAs heterojunction of lower electron density, Kirpichev *et al.* observed signals shifted from the laser line by integer multiples of the electron cyclotron energy $\hbar\omega_c$ which were shown to result from hot magnetophotoluminescence, the recombination of hot electrons and heavy holes in the bulk of the GaAs.[25,26] In the present measurements, however, the origin of the observed signal may be confirmed as two dimensional from a comparison of spectra measured in both the 45° and 0° orientations, shown in Fig. 6. We can see that the energies of the inter-Landau level SPE peaks depend on $B_\perp$ rather than the total magnetic field strength as would be the case for hot photoluminescence from bulk carriers.

The origin of the observed signal can also be determined from its variation with incident photon energy. Spectra measured at $B = 4$ and 8 T in the 45° orientation for a range of excitation energies E_L are shown in Fig. 7. At $B = 4$ T the form of the spectrum is essentially unchanged with decreasing excitation energy, as would be expected from Raman scattering, although there does appear to be some broad incoming resonance behavior, with the strongest signal observed for $E_L = 1.602$ eV ($\Delta = -30\,\mathrm{cm}^{-1}$). For $B = 8$ T the form of the spectrum changes more with excitation energy, although the underlying peak structure remains unchanged. The 2* mode at a Raman shift of $120\,\mathrm{cm}^{-1}$ appears to be strongly resonant, as are the features at 25 and $183\,\mathrm{cm}^{-1}$.

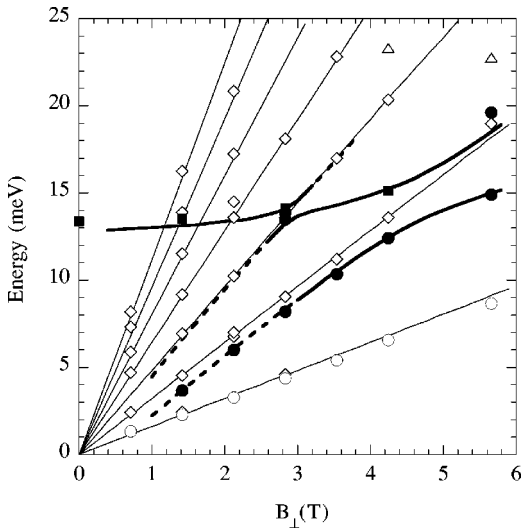

FIG. 5. Theoretical (lines) and experimental (symbols) excitation energies, as a function of $B_\perp$, the component of magnetic field normal to the plane of the 2DEG, for $q=1.145\times10^5\,\mathrm{cm}^{-1}$ (45° orientation). The energies of inter-Landau level excitations are indicated by the thin solid lines and of charge-density excitations by the thick solid and broken lines; the broken lines correspond to weaker Raman intensities, determined from the imaginary part of the charge-density response function. Charge-density excitation energies determined from the experimental spectra are indicated by the closed symbols: ●, depolarized, and ■, polarized Raman spectra. Experimental SPE inter-Landau level transition energies are indicated by the open symbols: ◇ (peaks of broad linewidth modes present in the experimental spectra for both polarizations) and ○ (narrow peak, more prominent in the depolarized spectra at low fields). △ indicate peaks possibly associated with an intersubband excitation, or with the maximum in the dispersion of a high-order magnetoplasmon.

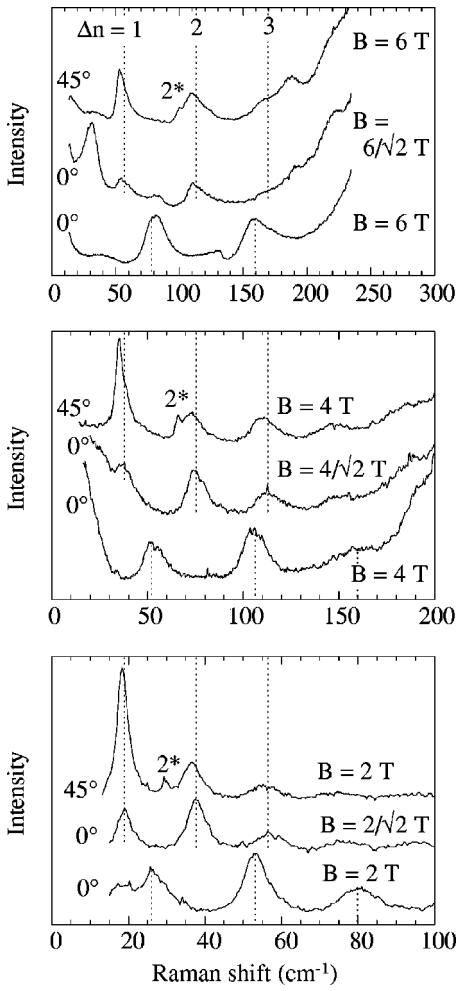

FIG. 6. Depolarized Raman spectra measured with the plane of the sample oriented both normal ($\theta=0°$) and at $\theta=45°$ to the magnetic field. The top two spectra in each panel correspond to the same component of the magnetic field normal to the plane of the 2DEG; the top and bottom spectra correspond to the same total magnetic field. The fact that the main peaks are present at the same Raman shifts in spectra measured in different orientations but with the same perpendicular component of magnetic field indicates that they result from inter-Landau level transitions in the 2DEG. Inter-Landau level transitions are indicated by changes in Landau level index Δn. 2* indicates a Bernstein mode.

There also appear to be two broad features, centered at $\Omega \sim 85$ and $155\,\mathrm{cm}^{-1}$, which do not seem to shift in absolute energy and could result from hot photoluminescence.

Further confirmation of the Raman nature of the inter-Landau level peaks signals is given by the linear variation of their intensities with incident power density, which was varied between 0.1 and 1 $\mathrm{kW\,cm}^{-2}$ (although note that the electron temperature will be less than 40 K for the lower powers). In conclusion, these peaks may therefore be unambiguously identified as resulting from Raman scattering by inter-Landau level excitations in the quantum well and not hot magnetophotoluminescence in the bulk. The fact that the energy dispersion of these peaks with magnetic field is in good agreement with that of inter-Landau level SPE's lends support to their assignment as single-particle-like in origin. However, counter to this, we should note that these inter-Landau level peaks are significantly stronger than predicted from calculations of the SPE Raman spectrum from the free electron polarizability [Eqs. (1) and (4)], which predict that for finite q a peak due to the $\Delta n=1$ transition should be dominant, with a rapid reduction in intensity with increasing Δn. This can be seen from a comparison of such theoretical SPE spectra for $B=2$ and 4 T, shown in Fig. 8, with the experimental spectra for these fields in Figs. 3 and 4. In addition, the inter-Landau level peaks develop structure and increase in width with increasing magnetic field and with increasing order Δn of the inter-Landau level transition. This broadening appears to be approximately linear with B, as can be seen in Fig. 3, and is in contrast to the behavior of the 2* peak, the width of which appears to be independent of B. We will return to the question of the nature of these inter-Landau level excitations and a discussion of the anomolous intensity and the width of the Raman peaks in Sec. VII.

We should also note that there appear low-frequency peaks in the high-field spectra in Figs. 4 and 6, at lower energies than that of the first inter-Landau level transition. This is particularly prominent at $30\,\mathrm{cm}^{-1}$ for $B=4.243\,\mathrm{T}=6/\sqrt{2}\,\mathrm{T}$ in the 0° orientation. A less intense peak also occurs at the same Raman shift in the $B=6$ T spectrum for the 45° orientation, suggesting that this feature is associated with Raman scattering from the 2DEG, and at a slightly higher frequency for $B=6$ T in the 0° orientation. The origin of these peaks is not clear, but they are probably associated

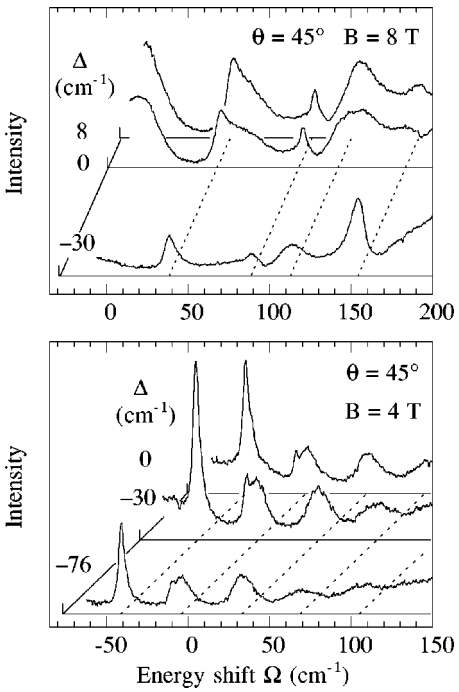

FIG. 7. Depolarized Raman scattering spectra measured in the 45° orientation, with applied magnetic fields of 4 T and 8 T, for various excitation wavelengths. The incident photon energy is expressed as a detuning Δ from 1.598 eV and the scattered photon energy is given as a Stokes energy shift Ω from this value (i.e., the Raman shift is $\Omega-\Delta$). The main features observed occur at a constant Raman shift, supporting their assignment to inter-Landau level transitions. It is possible that the broad features observed in the 8 T spectra at $\Omega=85$ and 155 cm^{-1} result from hot photoluminescence.

with intra-Landau level excitations.

VI. BERNSTEIN MODES

As already identified in the previous section, the spectra for $q=1.15\times10^5\ \mathrm{cm}^{-1}$ in Fig. 6 also reveal the presence of a narrow line (labeled 2*), on the low-energy side of the $\Delta n=2$ peak, which is not present in the $q=0$ spectra. A comparison of the polarized and depolarized spectra in Fig. 4 indicates that this mode 2* is present only in depolarized Raman scattering. In the polarized spectrum for $B=6$ T a shoulder (labeled MP) is present on the high-energy side of the $\Delta n=2$ inter-Landau level transition.

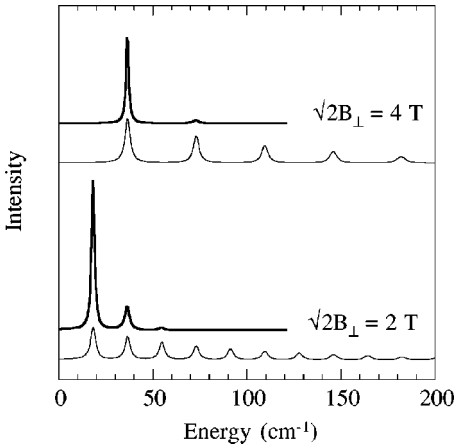

FIG. 8. Theoretical SPE Raman spectra determined with Eq. (1) from the electronic polarizability $\chi_0(q,\omega)$ for magnetic field strengths $B_\perp=1.414$ and 2.828 T perpendicular to the plane of the 2DEG (cf. the $\theta=45°$ experimental spectra for $B=2$ and 4 T in Fig. 4). Wave-vector-conserving spectra (thick lines) determined for $q=1.145\times10^5\ \mathrm{cm}^{-1}$, and wave vector breakdown spectra (thin lines) determined using Eq. (10) with $\Delta q=2\times10^5\ \mathrm{cm}^{-1}$, are shown.

The energies of these modes, 2* and MP, are plotted in Fig. 5 as a function of $B_\perp=B/\sqrt{2}$, the perpendicular component of the magnetic field, where they are compared with the energies of the charge-density excitations of the 2DEG determined within the RPA. The theoretical energies have been determined from the peaks in the Raman spectra calculated using the charge-density response function χ_ρ [Eq. (2)]. Excellent agreement is obtained between experiment and theory for the B-field dependence of these modes and, in particular, the magnetic field independent shift of 0.8 meV ($B_\perp<4$ T) of the 2* mode below the $\Delta n=2$ SPE is well reproduced. This mode (which was assigned to a spin-density excitation in Ref. 5) is therefore a Bernstein mode, resulting from a nonlocal interaction between the plasmon and the first harmonic of the cyclotron resonance.[27–30] The anticrossing at $B_\perp\sim5$ T, where the magnetoplasmon would cross the $\Delta n=2$ SPE energy, is also observed in experiment, with the peak MP assigned to the higher-energy magnetoplasmonlike mode.

To give an indication of oscillator strength, only those modes above a certain threshold intensity have been included; the dashed lines indicate peaks with a slightly lower threshold than those indicated by the solid lines. An electron density of $1.2\times10^{12}\ \mathrm{cm}^{-2}$ has been assumed in order to give agreement for the energy of the $B=0$ plasmon, and the electron temperature and phenomenological damping γ have been determined from the $B=0$ SPE line shape, but otherwise there are no free fitting parameters; the effects of nonparabolicity on the Landau level energies have been taken into account by Eq. (7). Note, however, that the Raman intensity of the lower-energy Bernstein mode 2*, determined from the imaginary part of χ_ρ, is predicted to become small at small magnetic fields away from the anticrossing, whereas this mode, observed in depolarized scattering, is still strong and well defined in the experimental spectra.

The variation with ql_0 of the RPA charge-density excitation energies for $B_\perp=1.414$ and 4.243 T (corresponding to $B=2$ and 6 T, respectively, for the 45° orientation) is shown in Fig. 9; for $B_\perp=1.414$ T, $l_0=216$ Å and for $B_\perp=4.243$ T, $l_0=125$ Å. The experimentally determined energies are also indicated. In Fig. 9(a) the dominant mode follows the classical magnetoplasmon dispersion of the form

$$\omega=\sqrt{\omega_c^2+\omega_p(q)^2}. \tag{9}$$

$\hbar\omega_c$ is the energy of the $\Delta n=1$ transition and $\omega_p(q)$ is the plasmon frequency for wave vector q at $B=0$; $\omega_p(q)\propto q^{1/2}$ in the long-wavelength limit. In addition to this magnetoplasmon mode there is also a much weaker series of Bernstein modes, the first of which appears to account for the mode 2* observed in depolarized Raman scattering, as dicussed in the previous section. For the larger field $B_\perp=4.243$ T [Fig. 9(b)] the charge-density excitation spectrum has evolved into a series of Bernstein mode dispersions.[27] Note that as these

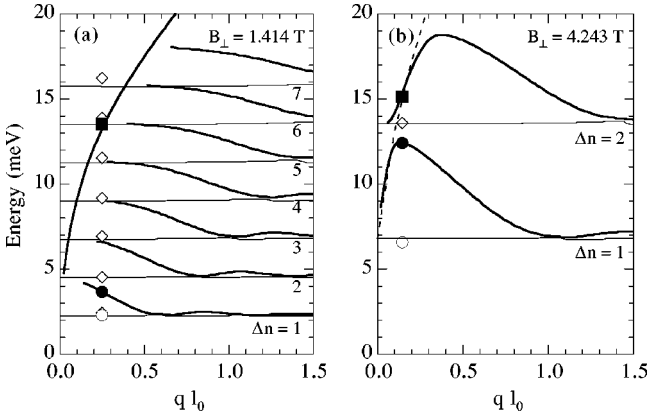

FIG. 9. Charge-density excitation dispersions with in-plane wave vector q calculated within the RPA for magnetic fields perpendicular to the plane of the 2DEG of (a) $B_\perp = 1.414$ T ($l_0 = 216$ Å) and (b) $B_\perp = 4.243$ T ($l_0 = 125$ Å). Only those modes above a threshold Raman intensity, determined from the imaginary part of the charge-density response function, are shown (thick lines). In (b) the broken line indicates the dispersion obtained using the classical expression for the magnetoplasmon energy ($\omega = \sqrt{\omega_c^2 + \omega_{p0}^2 q/q_0}$, where ω_c and ω_{p0} have been determined from experiment: ω_c is the energy of the $\Delta n = 1$ transition, ω_{p0} is the plasmon energy determined at $B = 0$ for wave vector $q_0 = 1.145 \times 10^5\ \mathrm{cm}^{-1}$). The thin lines indicate the energies of the peaks in the SPE spectrum determined from the imaginary part of the Mermin-corrected polarizability. Energies determined from Raman measurements performed in the 45° orientation ($q = 1.145 \times 10^5\ \mathrm{cm}^{-1}$) are indicated by the symbols (assignment as for Fig. 5): (a) $B = 2$ T and (b) $B = 6$ T.

calculations have been performed within the RPA, exchange-correlation is not included and so the form of these dispersions at large wave vectors should be treated with caution. Nevertheless, they provide a useful picture of the charge-density modes in this system. In particular, the anticrossing of the magnetoplasmon with the $\Delta n = 2$ SPE mode can be readily seen in Fig. 9(b) to be associated with a maximum in the Bernstein mode dispersion. For comparison, the magnetoplasmon dispersion predicted using Eq. (9) is also indicated. Note that some authors describe the lowest Bernstein mode as a magnetoplasmon[15]; here this term will be reserved for a mode following the classical dispersion given in Eq. (9).

We should note at this stage that the well-defined nature of these q-dependent charge-density modes in the experimental spectra, and the fact that they are not present for $q = 0$, indicates that their observation results from a wave-vector-conserving Raman mechanism.

VII. BREAKDOWN OF WAVE-VECTOR CONSERVATION

Although the energies of the broad peaks observed in both polarized and depolarized experimental spectra agree well with the SPE transition energies between Landau levels predicted by theory, and the peaks are confirmed as Raman in nature, we have not yet accounted for the intensity and broadening of these peaks. In particular, from calculations of SPE Raman spectra from the free electron polarizability, the relative strengths of the higher-order peaks are predicted to decrease with increasing B and decreasing q, with Raman scattering from all inter-Landau level SPE's expected to be forbidden for $q = 0$, whereas, even in the $q = 0$ experimental spectra (see Fig. 6), strong inter-Landau level peaks of comparable intensity are observed. Examples of calculated spectra for the 45° orientation are given in Fig. 8 (thick lines) for $B = 2$ and 4 T, which may be compared with corresponding experimental spectra in Fig. 4.

The presence of these strong inter-Landau level modes in the Raman spectra can be ascribed to a Raman scattering process in which wave vector is not conserved, as suggested in the context of Raman measurements in the integer and fractional quantum Hall regimes.[1–3,31] Such a breakdown of wave vector conservation could result from fluctuations in the confining potential, associated with remote ionized impurities (the spacer layer thickness is only 100 Å in the present sample) or well width fluctuations. If we first assume that these peaks are a result of Raman scattering by SPE's, Raman spectra may be calculated within a simple phenomenological model[32,33] employing a characteristic breakdown wave vector Δq:

$$R_{\mathrm{SPE}}(\omega) \propto -[N(\omega)+1] \int \mathrm{Im}[\chi_0(q,\omega)] \frac{1}{q^2 + \Delta q^2} dq. \tag{10}$$

Raman spectra calculated using Eq. (10) with $\Delta q = 2 \times 10^5\ \mathrm{cm}^{-1}$ are also shown in Fig. 8. The relative intensities of the inter-Landau level peaks are indeed much closer to those observed experimentally, even for this moderate in-plane wave vector Δq. This value of Δq corresponds to a length scale for fluctuations in the quantum well potential of ~ 500 Å, of comparable magnitude to the cyclotron radius for the magnetic fields considered here, suggestive of a magnetic field induced localization of the electron states in the quantum well.

However, comparison of the spectra in Figs. 4 and 8 indicates that the simple model of Eq. (10) has failed to account for the increasing width of the inter-Landau level peaks with increasing magnetic field. It is possible that the structure and width of the peaks may be attributed in part to the complex spin split nature of the conduction subband, arising from the interplay between the Zeeman and the intrinsic bulk inversion asymmetry and Rashba spin splitting in a tilted magnetic field.[21,34] However, the results of Ref. 21 would suggest that the spin-splitting should be much less than the observed widths of the inter-Landau level peaks. It should be noted that conduction band nonparabolicity, which leads to an unequal spacing of Landau levels, has been included in the calculations presented in Fig. 8; although this does lead to some broadening of the inter-Landau level SPE peaks with increasing inter-Landau level order Δn, it is clearly not sufficient to explain the observed peak widths at large B.

Apart from the effects of nonparabolicity, the linewidths of the calculated peaks in Fig. 8 are essentially determined by the single-particle damping γ in Eq. (4), which is kept constant (0.2 meV) in the above calculations. As the width of the long-wavelength q-conserving collective excitation 2* appears to be relatively unaffected by magnetic field, this would suggest that the single-particle lifetime of the extended states in the Landau quantized 2DEG is well described by a B-independent γ. However, in the case of com-

plete breakdown of wave vector conservation, the Raman spectrum for SPE's may be taken as representing the single-particle Landau level density of states, which includes all states (localized and extended). In this case the peak linewidths will provide a measure of the Landau level broadening Γ, which has indeed been observed by some authors to increase with magnetic field (as $B^{1/2}$ in accordance with the model of Ando and Uemura[35]) although others have found Γ to be independent of B.[36]

Finally, further investigation of Figs. 4 and 6 reveals in the depolarized spectra measured at finite q the presence of a narrow peak, superimposed on the $\Delta n=1$ inter-Landau level transition, which is not present for $q=0$ and emerges in the finite q polarized spectra only at high magnetic fields. This feature may correspond to the wave-vector-conserving peak expected for the $\Delta n=1$ inter-Landau level SPE transition for finite q, as shown in Fig. 8. Furthermore, the $\Delta n=2$ inter-Landau level peaks observed in the depolarized spectra in Fig. 4 are more intense than in the corresponding polarized spectra, whereas the higher-order inter-Landau level peaks are of comparable intensity for the two polarization configurations. This suggests that the weak $\Delta n=2$ SPE feature predicted by theory for $q=1.15\times10^5\ \mathrm{cm}^{-1}$ for the magnetic field strengths considered here (see Fig. 8) may contribute to the observed intensity of the $\Delta n=2$ inter-Landau level peak observed in the depolarized spectra. Therefore, it appears that wave-vector-conserving Raman scattering from SPE's may also be observed at high magnetic field in the depolarized spectra.

VIII. CHARGE-DENSITY EXCITATION DENSITY OF STATES

Instead of Raman scattering by SPE's, it may be that the inter-Landau level peaks result from a non-q-conserving Raman mechanism involving charge-density excitations; i.e., the spectra will then essentially represent the density of states of the Bernstein modes [or a density of states weighted by some wave vector breakdown term, such as that given in Eq. (10)]. This could also account for the increasing width of the peaks, as the Bernstein mode dispersions cover an energy range comparable to the inter-Landau level spacing, as can be seen in Fig. 9. However, counter to this we should note that the observed peak energies are well reproduced assuming that they are SPE's, whereas we would expect the peaks in the Bernstein mode density of states to occur at higher energies than those of the inter-Landau level transitions.

Nevertheless, the forms of the high-field spectra in Figs. 4 and 6 are suggestive of non-q-conserving Raman scattering from charge-density excitations. In Fig. 10 spectra measured at $B=8$ T in the 45° orientation ($B_\perp=5.657$ T) are compared with the calculated magnetoplasmon dispersions. In particular, the asymmetric line shape observed on the high-energy side of the $\Delta n=1$ transition, with a peak at ~15 meV, may reflect the density of states of the Bernstein mode; the high-energy cutoff of this feature corresponds well to the energy of the maximum in the calculated $\Delta n=1$ charge-density dispersion. Similarly, a strong asymmetric peak at ~23 meV (most prominent in the depolarized spectrum measured at $E_L=1.602$ eV) could correspond to the maximum in the $\Delta n=2$ charge-density dispersion. Note that the Bernstein mode 2*, which is present only in the depolarized spectrum measured at $E_L=1.598$ eV, occurs at a slightly lower energy than the peak of the feature in the polarized spectrum attributed to the $\Delta n=1$ density of states line shape.

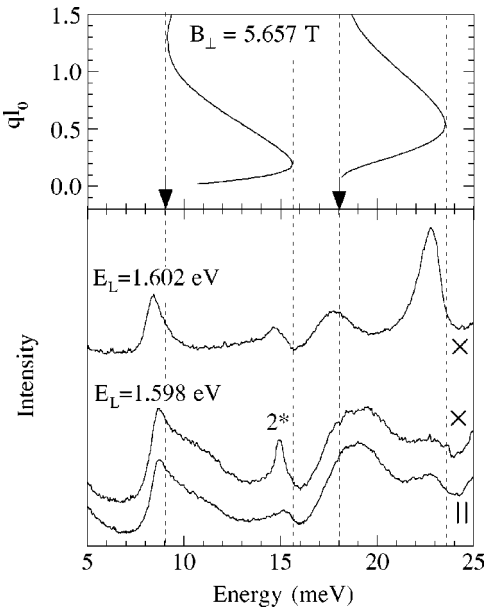

FIG. 10. Raman spectra measured with an applied magnetic field of 8 T in the 45° orientation (magnetic field component normal to the plane of the 2DEG $B_\perp=5.657$ T) for different incident laser energies E_L and polarizations ($\times$ depolarized, $\|$ polarized) are shown in the lower panel. The $\Delta n=1$ and 2 charge-density dispersions calculated within the RPA for $B_\perp=5.657$ T are shown in the top panel; the arrows indicate the inter-Landau level transition energies. It is proposed that the depolarized ($\times$) spectrum obtained with $E_L=1.602$ eV essentially represents the density of states of the charge-density excitations, with the asymmetric peaks at 14.8 and 22.8 meV corresponding to the maxima of the $\Delta n=1$ and 2 dispersions. These features also appear to be present in the spectra measured with $E_L=1.598$ eV, with the high-energy cutoff from the $\Delta n=1$ dispersion at 15.5 meV occurring just above the Bernstein mode (2*) present in the depolarized spectrum ($\times$).

IX. SUMMARY

In conclusion, a smooth transition has been observed in the inelastic light scattering spectrum from an electron gas confined in a GaAs quantum well, as it evolves from a two-dimensional system to a fully quantized system in the presence of an applied magnetic field. For moderate magnetic fields, $qv_F<\omega_c\ll E_F/\hbar$, corresponding to filling factors in the range 6 to 50, there is evidence for both wave-vector-conserving and nonconserving Raman scattering mechanisms from electronic excitations. In particular, wave-vector-conserving Raman scattering from the $\Delta n=2$ Bernstein modes has been observed in depolarized scattering. However, the intensity of this mode, which disperses with magnetic field at a constant energy shift below the bare SPE transition, is significantly greater than that predicted by simple linear response theory when far from the resonance

with the magnetoplasmon. There is also evidence for wave-vector-conserving Raman scattering by SPE's in the depolarized spectra. However, inelastic light scattering by inter-Landau level excitations (tentatively assigned to SPE's), in which there is no conservation of wave vector, dominates both the polarized and depolarized spectra, with a series of up to the $\Delta n = 7$ inter-Landau level transition observed. At high fields, the form of the Raman scattering spectra (again, both polarized and depolarized) can be identified with the density of states of charge-density excitations.

ACKNOWLEDGMENTS

I would like to express my thanks to the Royal Society and the U.K. EPSRC for support of this work. I am grateful to B. Etienne (Laboratoire de Microstructures et Microélectronique, CNRS) for the provision of the molecular beam epitaxial sample used in this work, R. T. Phillips for the use of an Oxford Instruments optical access magnet, and D. S. Kainth, H. P. Hughes, and B. Jusserand for valuable discussions.

[1] A. Pinczuk, B. S. Dennis, D. Heiman, C. Kallin, L. Brey, C. Tejedor, S. Schmitt-Rink, L. N. Pfeiffer, and K. W. West, Phys. Rev. Lett. **68**, 3623 (1992).
[2] A. Pinczuk, B. S. Dennis, L. N. Pfeiffer, and K. W. West, Phys. Rev. Lett. **70**, 3983 (1993).
[3] H. D. M. Davies, J. C. Harris, J. F. Ryan, and A. J. Turberfield, Phys. Rev. Lett. **78**, 4095 (1997).
[4] G. Brozak, B. V. Shanabrook, D. Gammon, and D. S. Katzer, Phys. Rev. B **47**, 9981 (1993).
[5] D. Richards, E. T. M. Kernohan, R. T. Phillips, and B. Etienne, in *Proceedings of the 23rd International Conference on the Physics of Semiconductors*, edited by M. Sheffler and R. Zimmermann (World Scientific, Singapore, 1996), p. 2319.
[6] B. Jusserand, D. Richards, H. Peric, and B. Etienne, Phys. Rev. Lett. **69**, 848 (1992).
[7] D. Richards, B. Jusserand. H. Peric, and B. Etienne, Phys. Rev. B **47**, 16 028 (1993).
[8] G. Abstreiter, M. Cardona, and A. Pinczuk, in *Light Scattering in Solids IV*, edited by M. Cardona and G. Güntherodt (Springer, Heidelberg, 1984), p. 5.
[9] M. Berz, J. F. Walker, P. von Allmen, E. F. Steigmeier, and F. K. Reinhart, Phys. Rev. B **42**, 11 957 (1990).
[10] B. Jusserand, D. Richards, G. Allan, C. Priester, and B. Etienne, Phys. Rev. B **51**, 4707 (1995).
[11] D. Richards and B. Jusserand, Phys. Rev. B **59**, R2506 (1999).
[12] D. Richards, J. Wagner, and J. Schmitz, Solid State Commun. **100**, 7 (1996).
[13] C. Bulutay and M. Tomak, Phys. Rev. B **54**, 14 643 (1996).
[14] A. H. MacDonald, Phys. Rev. B **30**, 4392 (1984).
[15] C. Kallin and B. I. Halperin, Phys. Rev. B **30**, 5655 (1984).
[16] H. C. A. Oji and A. H. MacDonald, Phys. Rev. B **33**, 3810 (1986).
[17] A. Fainstein, T. Ruf, M. Cardona, V. I. Belitsky, and A. Cantarero, Phys. Rev. B **51**, 7064 (1995).
[18] N. D. Mermin, Phys. Rev. B **1**, 2362 (1970).
[19] U. Ekenberg, Phys. Rev. B **40**, 7714 (1989).
[20] F. Malcher, G. Lommer, and U. Rössler, Superlattices Microstruct. **2**, 267 (1986).
[21] P. Pfeffer, Phys. Rev. B **55**, R7359 (1997).
[22] H. Peric, B. Jusserand, D. Richards, and B. Etienne, Phys. Rev. B **47**, 12 722 (1993).
[23] T. Ando, J. Phys. Soc. Jpn. **44**, 475 (1978).
[24] D. S. Kainth, D. Richards, H. P. Hughes, M. Y. Simmons, and D. A. Ritchie, J. Phys.: Condens. Matter **12**, 439 (2000).
[25] V. E. Kirpichev, I. V. Kukushkin, B. N. Shepel', K. von Klitzing, and K. Eberl, Pis'ma Zh. Éksp. Teor. Fiz. **62**, 863 (1995) [JETP Lett. **62**, 877 (1995)].
[26] V. E. Kirpichev, I. V. Kukushkin, B. N. Shepel', K. von Klitzing, and K. Eberl, Pis'ma Zh. Éksp. Teor. Fiz. **63**, 974 (1996) [JETP Lett. **63**, 1031 (1996)].
[27] N. A. Krall and A. W. Trivelpiece, *Principles of Plasma Physics* (McGraw-Hill, New York, 1973).
[28] E. Batke, D. Heitmann, J. P. Kotthaus, and K. Ploog, Phys. Rev. Lett. **54**, 2367 (1985).
[29] T. Zettler, C. Peters, J. P. Kotthaus, and K. Ploog, Surf. Sci. **229**, 388 (1990).
[30] D. E. Bangert, R. J. Stuart, H. P. Hughes, D. A. Ritchie, and J. E. F. Frost, Semicond. Sci. Technol. **11**, 352 (1996).
[31] A. O. Govorov, Zh. Éksp. Teor. Fiz. **112**, 1041 (1997) [JETP **85**, 565 (1997)].
[32] D. Olego and M. Cardona, Solid State Commun. **32**, 375 (1979).
[33] I. K. Marmorkos and S. Das Sarma, Phys. Rev. B **45**, 13 396 (1992).
[34] A. O. Govorov, Phys. Low-Dim. Struct. **3**, 71 (1996).
[35] T. Ando and T. Uemura, J. Phys. Soc. Jpn. **36**, 959 (1974).
[36] A. Potts, R. Shepherd, W. G. Herrenden-Harker, M. Elliott, C. L. Jones, A. Usher, G. A. C. Jones, D. A. Ritchie, E. H. Linfield, and M. Grimshaw, J. Phys.: Condens. Matter **8**, 5189 (1996).